Divergence Distance Based Index for Discriminating Inrush and Internal Fault Currents in Power Transformers

Divergence Distance Based Index for Discriminating Inrush and Internal Fault Currents in Power Transformers

Mohsen Tajdinian and Haidar Samet, *Member, IEEE*

***Abstract*—This article puts forward a new algorithm based on Kullback–Leibler divergence (KLD) for discriminating inrush and internal fault currents in power transformers. Specifically, the main idea of this algorithm is to utilize the current signal discrepancy of the distribution with ideal fault current waveforms. To such an aim, the proposed index reproduces the differential current signal. Utilizing fast modified least squares technique, the differential current signal is generated. Applying the reconstructed differential current and ideal sinusoidal waveforms to the KLD indicator, the distribution discrepancy of the current signal from ideal sinusoidal waveform discriminates inrush and internal fault currents. Also, the internal/external identification index is introduced that utilizes the phase content of the signals from current transformers (CTs) on both sides to distinguish internal and external faults, especially the faults accompanied with CT saturation. As a result, the proposed method can distinguish inrush currents, internal and external fault currents with/without CT saturation, and internal fault currents during transformer energization. The performance of the proposed index is evaluated using practically recorded data and is further compared with the state of the art.**

***Index Terms*—Differential protection, Kullback–Leibler divergence (KLD), power transformer.**

I. Introduction

BEING costly as well as strategic components in the power grids, power transformers are known as one of the most important power system components. As a result, a special protection scheme known as differential protection unit is provided to protect the power transformers against internal failures. Owning to considerable differential currents, differential relays may mal-operate during power transformer energization currents or so-called inrush currents [1]. Obviously, differential relays should be able to quickly, accurately, and reliably discriminate inrush currents from fault signals to avoid false trips of the differential relays.

To identify magnetization inrush currents from fault conditions, several approaches have been proposed. The state-of-the-art approaches are grouped and described as follows.

1) *Harmonic restrain methods [1], [2]:* This approach is known as the most straightforward and simple approach, which contains noncomplex algorithms that operate based on the second and fifth harmonic currents for discrimination of the inrush current from fault current. It has been acknowledged that due to the modern core materials for power transformers, the harmonic contents may change, and as a result, the discrimination between an internal fault and inrush current becomes more difficult.
2) *Flux restrain and inductance-based methods [1], [3], [4]:* These methods depend on transformer parameters, and calculate the flux restrains, induced voltage, and also instantaneous inductance for the discrimination. However, the requirement of higher costs for accessories, including different search coils and depending on the transformer parameters, makes these algorithms less attractive.
3) *Patten recognition and artificial intelligence methods [5]–[8]:* These algorithms are based on pattern recognition principles and are implemented with neural networks and fuzzy logic. These algorithms are required to be retrained for building new models upon change of test system.
4) *Time-frequency analysis method [9]–[17]:* These algorithms utilize wavelet transform, which gives a more comprehensive overview of both time and frequency domains simultaneously. However, they need long data windows and are susceptible to noise as well as unanticipated disturbances.
5) *Ratio-based methods [18]–[20]:* These innovative methods are known as ratio-based methods and utilize both current-voltage signals for the discrimination of inrush currents and fault signals. However, sensitivity to the decaying dc component, dependence on both current and voltage information, and inherent one-cycle delay due to the utilization of discrete Fourier transform are the main drawbacks of such methods.

Manuscript received August 26, 2020; revised November 24, 2020, March 14, 2021, and April 13, 2021; accepted May 7, 2021. Date of publication May 25, 2021; date of current version January 7, 2022. *(Corresponding author: Haidar Samet.)*

Mohsen Tajdinian is with the School of Electrical and Computer Engineering, Shiraz University, Shiraz 71946-84636, Iran (e-mail: tajdinian.m@shirazu.ac.ir).

Haidar Samet is with the School of Electrical and Computer Engineering, Shiraz University, Shiraz 71946-84636, Iran, and also with the Department of Electrical Engineering, Eindhoven University of Technology, 5612 AZ Eindhoven, The Netherlands (e-mail: samet@shirazu.ac.ir, h.samet@tue.nl).

Color versions of one or more figures in this article are available at https://doi.org/10.1109/TIE.2021.3082071.

Digital Object Identifier 10.1109/TIE.2021.3082071

6) *Statistical and similarity-based methods [21]–[25]:* These algorithms utilize statistical momentums and similarity indices to discriminate between inrush currents and internal faults. Similar to ratio-based methods, these methods are sensitive to decaying dc components and may experience long delays in hard cases.

In all the mentioned approaches, fast and reliable decision-making and simultaneously dealing with the internal fault accompanied by current transformer (CT) saturation, the inrush current accompanied by high remanence, inrush currents, and internal faults and external fault [26]–[28] are the most challenging for the fault detections algorithms to deal with.

This article proposes an index based on the Kullback–Leibler divergence (KLD), which tries to discriminate inrush currents from internal faults utilizing discrepancy between the probability distributions of the reconstruction waveforms of the differential current signal and the ideal sinusoidal waveform. The main contributions of the proposed method are as follows.

1) The discrimination is performed using the comparison between the reconstructed waveform of the differential current signal and a sinusoidal waveform. To make a comparison, the KLD-based indicator is proposed to measure the distribution discrepancy between the two latter waveforms. Note that each reconstruction waveform of the differential current signal corresponds to a sliding window with a limited number of samples (ten samples considering a 100 sampling rate/cycle). During inrush, the signal comprises higher order harmonic components, which lead to variations in the reconstructed waveform corresponding to each window and consequently in the probability distribution as well.
2) To reconstruct the differential current signal, the fast modified least squares technique (MLSE) is employed. Note that to calculate the current waveform, fast waveform reconstruction is applied based on the limited number of samples. As a result, unlike [23], it does not require full-cycle data sampling for calculating the current signal. Also, unlike the suggested method in [23], the reconstruction of the waveform using MLSE reduces the impact of the dc component on the reconstructed waveform.
3) Due to the low latency, the proposed indicator can be calculated within the unsaturated region, as well as in the deep saturation condition. As a result, unlike [25], the proposed algorithm does not require extra algorithms for the identification of CT saturation.

The rest of this article is organized as follows. Section II introduces the proposed algorithm fundamental analysis. Section III provides the information that is required for implementing the proposed method. Sections IV describes the performance evaluation. Finally, Section V concludes this article.

II. Proposed Algorithm

In the following, the definition of KLD, the waveform reconstruction procedure and, finally, the proposed index for the discrimination of the inrush and internal fault currents are presented.

A. KLD Definition

Originating from information theory, KLD has been introduced as a probabilistic measure to find the discrepancy between two probability density functions over the same random variable. KLD measures the divergence of $q(x)$ from $p(x)$ as follows [29]:

$$\mathrm{KLD}\left(p\left(x\right),q\left(x\right)\right)=\sum_{x\in C}p\left(x\right)\log\frac{p\left(x\right)}{q\left(x\right)} \tag{1}$$

where it is assumed that $p(x) > 0$ and $q(x) > 0$ for any random variable x in probability space X. Since before/after fault inception, the power system current signal contains fundamental frequency sinusoidal component, $p(x)$ is selected as the probability distribution of a full cycle sinusoidal signal, which is defined as follows:

$$i_n(t)=\sin(2\pi ft) \tag{2}$$

where $i_n(t)$ and f are current signal and system frequency, which is selected as 50 Hz. It is assumed that $q(x)$ is the probability distribution of the reconstructed current signal $i_r(t)$, which has the following general expression:

$$i_r(t)=I_r\sin(2\pi ft-\theta). \tag{3}$$

As a result, KLD is rewritten as follows:

$$\mathrm{KLD}\left(p\left(i_n(t)\right),q\left(i_r(t)\right)\right)=\sum_{t\in T}p\left(i_n(t)\right)\log\frac{p\left(i_n(t)\right)}{q\left(i_r(t)\right)}. \tag{4}$$

Note that the reconstructed current signal $i_r(t)$ will be obtained from fault current.

B. Reproducing Differential Fault Current

During fault condition, it is assumed that the fault current is expressed as follows [1]:

$$i_{\mathrm{fault}}\left(t\right)=\ I_{\max}cos\left(\omega_0t-\theta\right)+I_{\mathrm{DC}}e^{-t/\tau} \tag{5}$$

where $I_{\max}$, ω_0 ,θ, and $\tau$are maximum fault current, frequency, phase angle, and time constant, respectively. By substituting the first-order Taylor expansion of $e^{-t/\tau}$in expression (5), the fault current is approximated as follows:

$$\begin{aligned}i_{\mathrm{fault}}\left(t\right)\approx\ I_{\max}cos\left(\omega_0t\right)cos\left(\theta\right)+I_{\max}\sin\left(\omega_0t\right)\sin\left(\theta\right)\\ +I_{\max}\cos\left(\theta\right)-\frac{I_{\max}\cos(\theta)}{\tau}t.\end{aligned} \tag{6}$$

To solve (6), it is suitable to discretize and rewrite the equation in matrix format as follows:

$$\left[I_{\mathrm{fault},i}\right]_{m\times1}=\left[K\right]_{m\times4}\times\left[X\right]_{4\times1} \tag{7}$$

where

$$\left[\mathrm{I}_{\mathrm{fault},i}\right]_{m\times1}=\left[\,i_{\mathrm{fault}}\left(t_1\right)\ i_{\mathrm{fault}}\left(t_2\right)\cdots\ i_{\mathrm{fault}}\left(t_m\right)\right]^T \tag{8}$$

$$\left[X\right]_{4\times1}=\left[\,I_{\max}cos\left(\theta\right)\ I_{\max}\sin\left(\theta\right)\ I_{\mathrm{DC}}\ -\frac{I_{\mathrm{DC}}}{\tau}\right]^T \tag{9}$$

$$\left[K\right]_{m\times4}=\begin{bmatrix}\cos(\omega_0t_1) & \sin(\omega_0t_1) & 1 & t_1\\ \vdots & \vdots & \vdots & \vdots\\ \cos(\omega_0t_m) & \sin(\omega_0t_m) & 1 & t_m\end{bmatrix}. \tag{10}$$

The least squares technique is known as one of the powerful tools for solving (7), being able to estimate the unknown parameters as follows:

$$[X] = \left[\left[[K]^T [K]\right]^{-1} [K]^T\right] [I_{\text{fault},i}]. \tag{11}$$

Using (11), the phase angle is calculated, and consequently, the reconstructed sinusoidal signal $i_r(t)$ is generated using (3). To reach the authenticated solution form (11), the parameter m should be greater than four considering 100 samples per cycle. In this article, a sliding data window with the length equal to ten samples is selected.

C. Proposed Algorithm for Discriminating Inrush and Internal Fault

Assume that *p(x)* is the distribution of a sinusoidal signal $i_n(t)$. Also, *q(x)* is the reconstructed sinusoidal signal $i_r(t)$ from the current waveform. The discrimination index, which is called the KLD index (KLDI), is defined as follows:

$$\text{KLDI} = \frac{\text{STD}\left\{\text{KLD}\left(p\left(i_n(t)\right), q\left(i_r(t)\right)\right)\right\}}{1 - \text{STD}\left\{\text{KLD}\left(p\left(i_n(t)\right), q\left(i_r(t)\right)\right)\right\}} \tag{12}$$

where STD denotes standard deviation. The KLDI functionality is based on the fact that for each window of the current sample if the reconstructed current signal remains unchanged, the KLD remains constant, and consequently, the KLDI value is almost zero. However, if the reconstructed current signal changes, KLD will change and as a result, the KLDI value would be notable.

D. Proposed Algorithm for Discriminating External and Internal Faults

As discussed, this article concentrates on discriminating inrush and internal fault currents. But for discriminating external and internal faults, Weng *et al.* [23] have shown that the phase content of the signals from CTs on both sides can be considered to distinguish internal and external faults, especially the faults accompanied with CT saturation. As stated in [23], during an internal fault, the currents of CTs are in phase, whereas during external faults, the currents of CTs are 180° out of phase. As a result, the internal/external identification (IEI) index is introduced as follows:

$$\text{IEI} = \frac{\left|\measuredangle i_{\text{CT},1}(t) - \measuredangle i_{\text{CT},2}(t)\right|}{180} \tag{13}$$

where $\measuredangle i_{\text{CT}}(t)$ denotes the phase angle of CT that is scaled between 0° to 180°. The IEI, defined as a normalized value, if varying between 0 to TH_1, can be used as an indication of internal faults. Contrarily, the variation of IEI between TH_2 and 1 can also be used as an indication of external faults.

III. Implementation

As shown in Fig. 1, the procedure of implementing the proposed algorithm contains five general stages. The stages are as follows.

1) The current samples are obtained by a 100 sample/cycle rate.

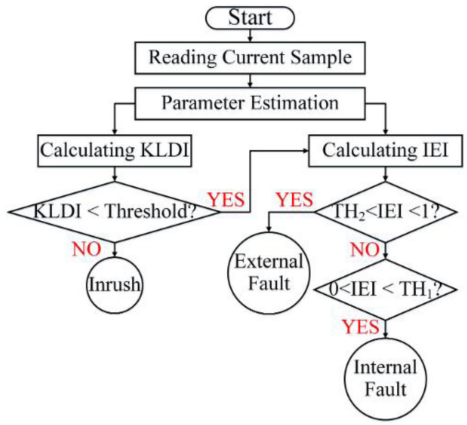

Fig. 1. Implementation procedure of the proposed index.

2) Parameter estimation: A sliding window containing ten current samples is fed to (7)–(11), to calculate the unknown parameters of (5).
3) Waveform reconstruction: Using (11), the magnitude and phase angle are calculated, and consequently, the reconstructed waveform is produced for one cycle using (3).
4) Calculating KLDI: Using (12), KLDI corresponding to each sliding window is calculated. Note that to calculate the KLDI, the signals $i_n(t)$ and $i_r(t)$are reproduced for one cycle and their probability density functions are generated. A decision is made when KLDI exceeds the threshold for five consecutive sliding windows.
5) Calculating IEI: To discriminate internal and external faults, using (13), IEI is calculated and checked with corresponding thresholds to discriminate internal and external faults. A decision is made when IEI exceeds the threshold for five consecutive sliding windows.

Considering that the proposed method has been developed using the data from unsaturated interval for internal/external fault conditions, it is also necessary to ensure the capability of the proposed method to provide robust estimation in the case of deep saturation. Knowing the fact that deep saturation may occur within one-sixth cycle after fault inception [30], the proposed index should be able to deal with waveform reconstruction and decision-making using 15 samples (considering 100 samples/cycle) at the most to guarantee the immunity of the proposed method against CT saturation. Considering the aforementioned point regarding decision-making reliability, the immunity of the proposed method against deep CT saturation has been guaranteed by the selection of a sliding data window length of ten and five samples for the decision criterion.

IV. Performance Evaluation

In the following, the performance of the proposed index is evaluated and further compared with the well-known second harmonic restrain (SHR) [1], [2] algorithm. The performance evaluation is conducted based on the obtained data from the simulated test system and practical data. The simulated test system is shown in Fig. 2. The detailed information regarding the specifications of the transformer and the CTs are provided in the Appendix [31]. In the simulated scenarios, different switching

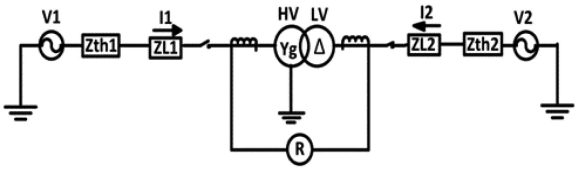

Fig. 2. Test system simulated in Power System Computer Aided Design (PSCAD).

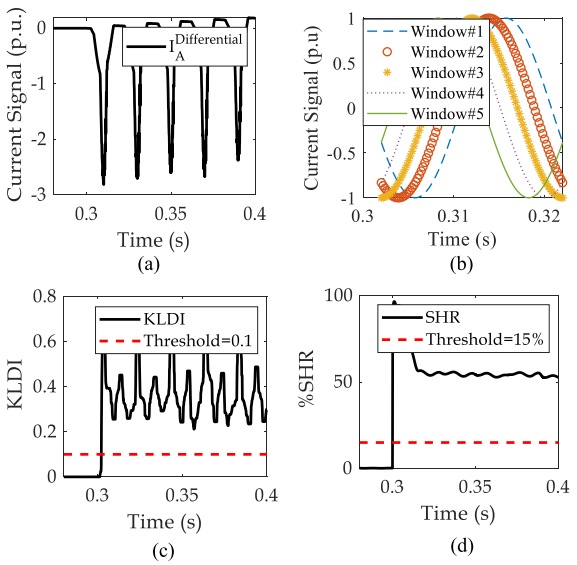

Fig. 3. Performance evaluation for inrush current signal. (a) Differential current signal. (b) Reconstructed sinusoidal waveform for five consecutive window data. (c) Proposed method. (d) SHR method.

instances with a range between 0 and 360°, fault resistance with a range between 0 and 5 Ω, fault inception angle with a range between 0 and 360°, and noise level with a range between 40 and 60 dB are considered. The threshold is obtained through "Otsu threshold algorithm" [32]. Note that in all cases, the threshold for the proposed index (KLDI) is considered 0.1. Also, the threshold for SHR is considered 15%, which is adopted from [21].

A. Simulation Results

1) Inrush Current: Fig. 3 shows the differential current for phase A ($I_A^{\text{Differential}}$) considering switching instance at $t = 300$ ms. As can be seen in Fig. 3(c) and (d), both methods successfully identify the inrush current. According to Fig. 3(b), it is evident that the reconstructed sinusoidal waveform mismatches for five consecutive data windows since the inrush current is not fitted on a standard sinusoidal waveform. As a result, the proposed index changes in time. Fig. 4 shows the differential current for phase A considering switching instance at $t = 306$ ms considering 30% remanent flux. While the SHR method shows unreliable response even after one cycle delay, the proposed method robustly distinguishes inrush current within less than a quarter of cycle after transformer energization.

2) Internal Fault: Applying a fault on 40% of the HV side of the transformer winding, the fault current is shown in Fig. 5. As can be seen in Fig. 5, both the proposed method and SHR can detect the fault signal. It should be noted that the proposed

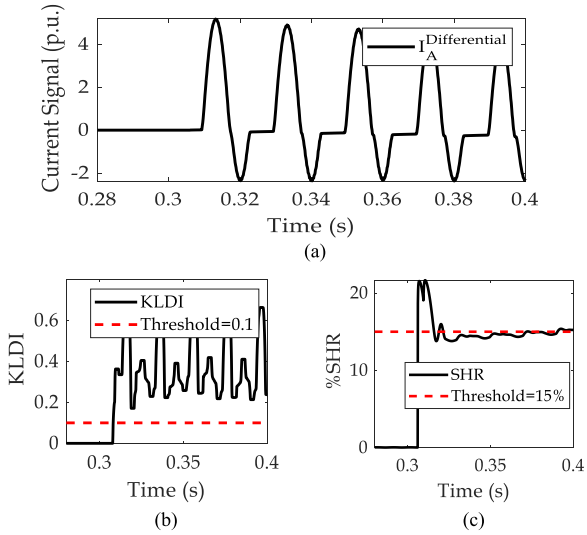

Fig. 4. Performance evaluation for inrush current signal with remnant flux. (a) Differential current signal. (b) Proposed method. (c) SHR method.

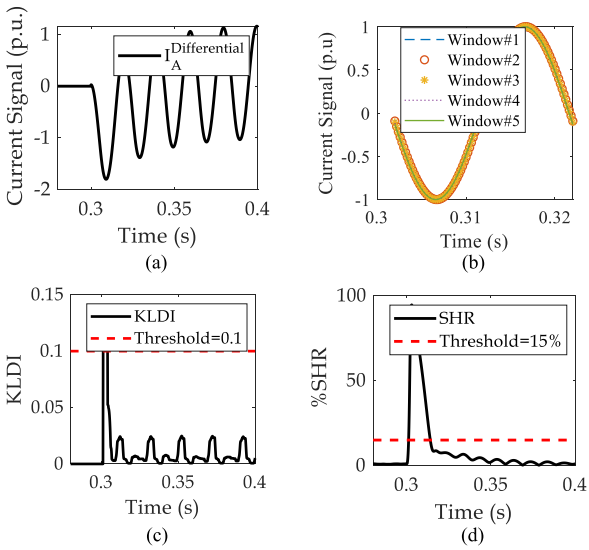

Fig. 5. Performance evaluation for internal fault signal. (a) Differential current signal. (b) Reconstructed sinusoidal waveform for five consecutive window data. (c) Proposed method. (d) SHR method.

method reaches below the threshold after almost 3 ms from the disturbance occurrence, whereas SHR identifies fault condition after 16 ms. As one can see in Fig. 5(b), the reconstructed sinusoidal waveform shows almost complete match for five consecutive window data. The complete match is due to the fact that the phase angle of the fault signal waveform is almost constant and as a result, the proposed index remains unchanged in time.

Fig. 6 demonstrates the performance evaluation for internal fault condition accompanied by CT saturation. According to Fig. 6(a), the current signal does not fit on a standard fault signal similar to (5) within the total time interval. As can be seen in Fig. 6(b), due to fast parameter estimation, the proposed index remains below the threshold during unsaturated interval, especially in the first quarter of cycle. Also, Fig. 6(b) reveals that

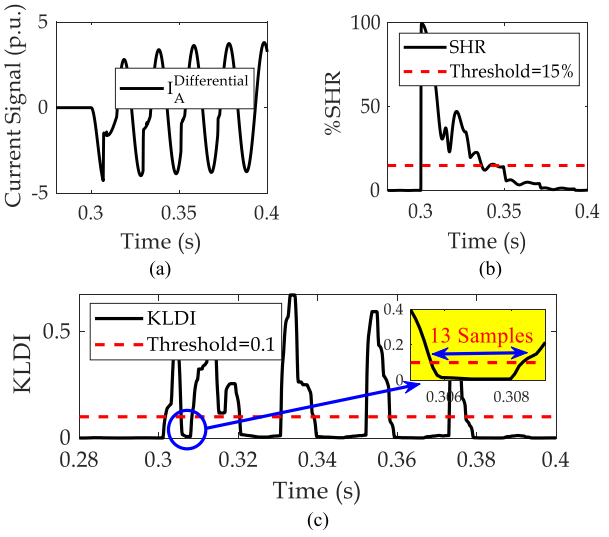

Fig. 6. Performance evaluation for internal fault signal accompanied by CT saturation. (a) Differential current signal. (b) Proposed method. (c) SHR method.

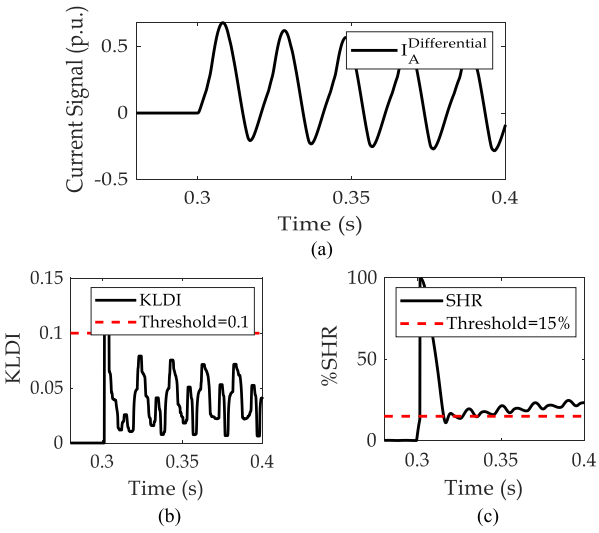

Fig. 7. Performance evaluation for transformer energization with an internal fault. (a) Differential current signal. (b) Proposed method. (c) SHR method.

once the signal becomes distorted, the proposed index quickly varies. On the contrary, the SHR algorithm utilizes a full-cycle window for performing calculations using the discrete Fourier transform. During saturation, the SHR algorithm's error is very large since the current signal does not fit on a standard fault signal similar to (5) within the total time interval. As a result, according to Fig. 6(c), the SHR algorithm experiences a large time delay to correctly identify faults accompanied by CT saturation.

3) Transformer Energization With an Internal Fault: The signal shown in Fig. 7 is the transformer energization with an internal fault condition that contains a minor 10% fault in the HV side of the power transformer. As can be seen in Fig. 7(b), the KLDI reaches below the threshold after about 3 ms, whereas according to Fig. 7(c), the SHR method fails to distinguish the inrush current. In the case of transformer energization with

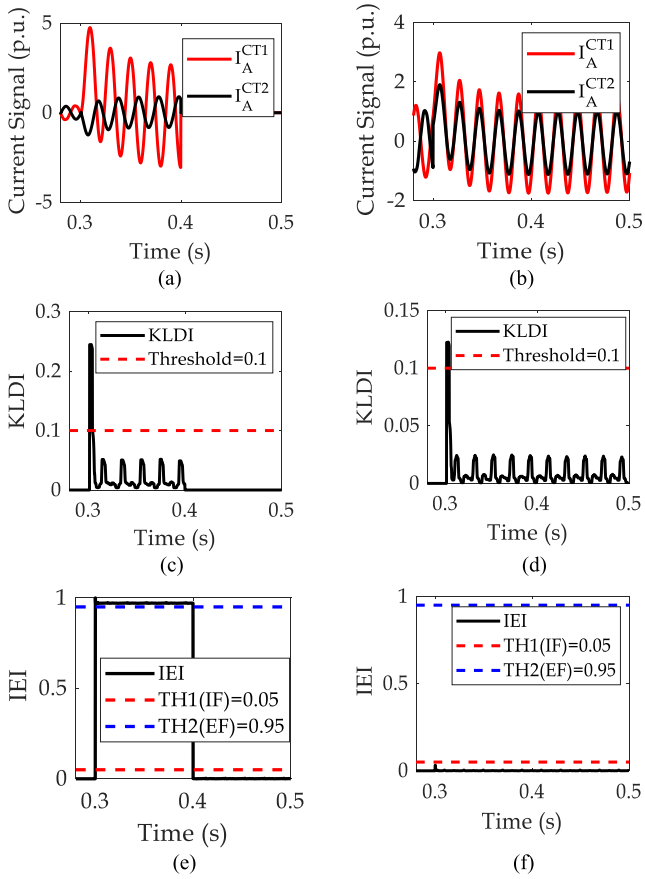

Fig. 8. Performance evaluation for external/internal fault current signals. (a) CT current signals for external fault. (b) CT current signals for internal fault. (c) Proposed KLDI for external fault. (d) Proposed KLDI for internal fault. (e) Proposed external/internal fault discrimination for external fault. (f) Proposed external/internal fault discrimination for internal fault.

internal fault, the current signal in the faulty winding does not reflect the inrush deformation and is more similar to the fault current than the inrush current [25]. As a result, the proposed method, which operates based on the waveform similarity to the sinusoidal signal, can successfully detect such minor faults in the power transformer.

4) External Fault: Fig. 8 provides performance evaluation for external/internal fault current signals.

In Fig. 8(a), I_A^{CT1} and I_A^{CT2}denote the current signal of phase A for the HV side of the transformer measured through (CT1) and the current signal of phase A for the LV side of the transformer measured through (CT2), respectively. Also, TH1(IF) and TH2(EF)denote the thresholds for identifying internal faults and external faults, respectively. As can be seen in Fig. 8, while KLDI identifies both fault signals, Fig. 8(e) shows that the current signals in Fig. 8(a) are almost 180° out of phase, and the IEI index value is close to 1. However, in Fig. 8(f), IEI index value is close to zero, which is in compliance with the in-phase condition shown in Fig. 8(b). Also, as one can see in Fig. 8(c) and (e), after fault clearance, both KLDI and IEI indices take zero value just after fault is cleared. The proposed index performs its analysis on the differential current signal that

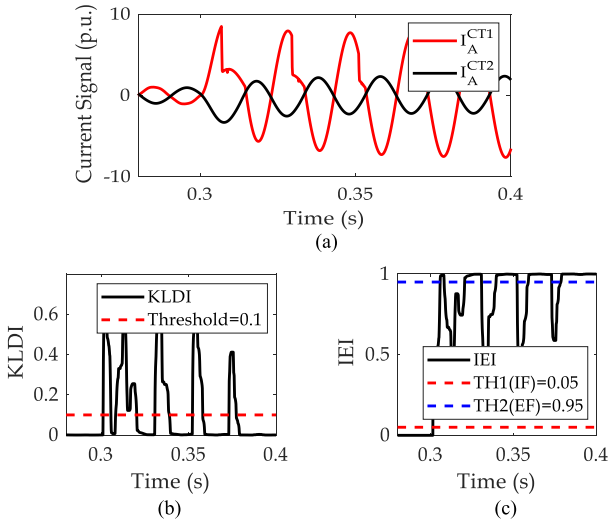

Fig. 9. Performance evaluation for external fault signal accompanied by CT saturation. (a) Differential current signal. (b) Proposed method. (c) Proposed external/internal fault discrimination for internal fault.

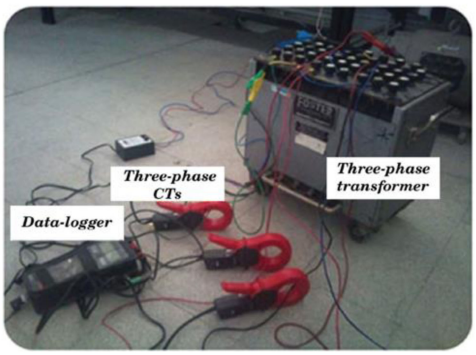

Fig. 10. Setup for producing and recording practical inrush and internal fault data.

triggers the operating current of the differential relay. After fault clearance, it is obvious that the operating current goes below the setting value for the operation of the differential relay. As a result, it is obvious that in such a circumstance the differential relay does not consider this circumstance as an internal fault.

In the case of an external fault accompanied by CT saturation, Fig. 9 shows that both KLDI and IEI indices successfully detect the external fault condition in about 3.4 ms after fault inception. It should be noted that both KLDI and IEI indices have values close to 1 in the unsaturated region [after 3.4 ms in Fig. 9(b) and (c)], and this condition provides almost ten consecutive samples to make a decision for the external fault inception. Considering the results given by the external fault scenario in Figs. 8 and 9, the proposed method can deal with the discrimination of internal/external faults.

B. Performance Evaluation With Practical Data

This section provides the performance evaluation of the proposed method with practical data. The laboratory setup for acquiring practical inrush and internal fault data is shown in Fig. 10. The power transformer nominal apparent power is 6

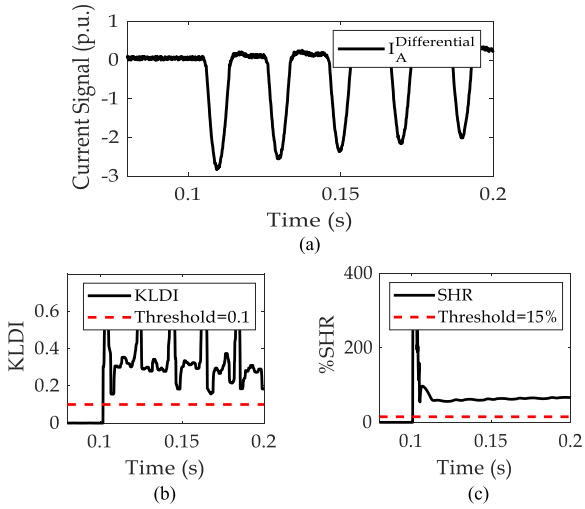

Fig. 11. Performance evaluation for practical inrush signal. (a) Differential current signal. (b) Proposed method. (c) SHR method.

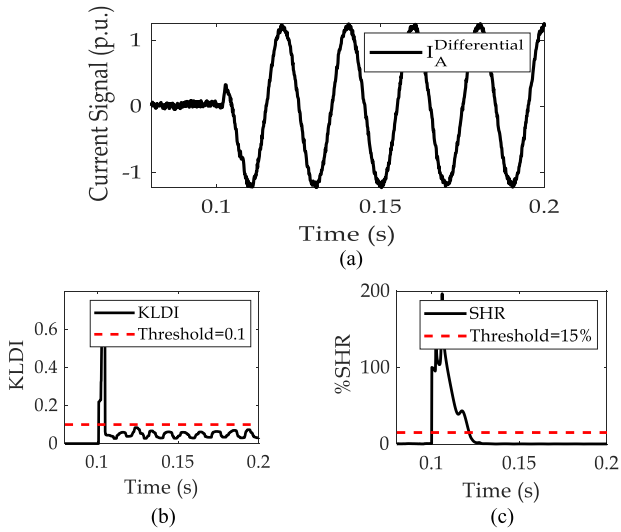

Fig. 12. Performance evaluation for practical internal fault signal. (a) Differential current signal. (b) Proposed method. (c) SHR method.

KVA and operates at 50 Hz, with the voltage ratio of 220/330 V. Note that the sampling time of the data logger is equal to 128 μs. Three cases contain an inrush current, an internal fault (minor 20% of winding to the ground), and an inrush current with an internal fault (minor 10% of winding to the ground) are presented in the following.

As can be seen in Figs. 11 and 12, both KLDI and SHR algorithms can successfully identify inrush and fault currents, respectively. As one can see in Figs. 11 and 12, KLDI requires less than 4 ms to reach the authenticated result, whereas for SHR, it takes about a full cycle to reach a valid result. According to Fig. 13, comparing the performance of KLDI and SHR algorithms in the case of dealing with inrush current with an internal fault, it can be concluded that the KLDI reaches below the threshold after about 4 ms, whereas the SHR method distinguishes fault current after one cycle unreliably.

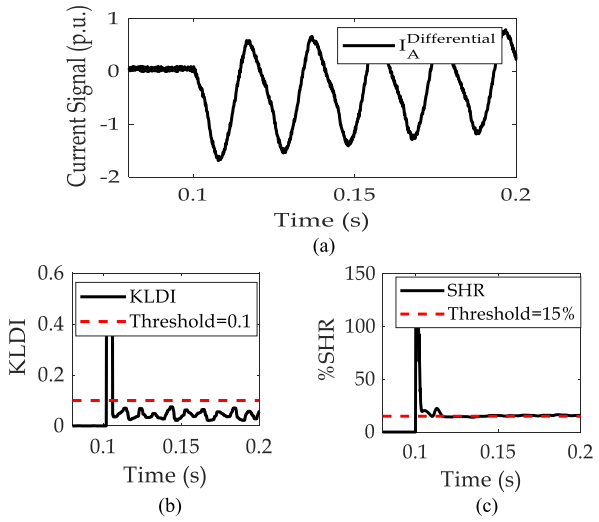

Fig. 13. Performance evaluation for practical inrush signal with an internal fault. (a) Differential current signal. (b) Proposed method. (c) SHR method.

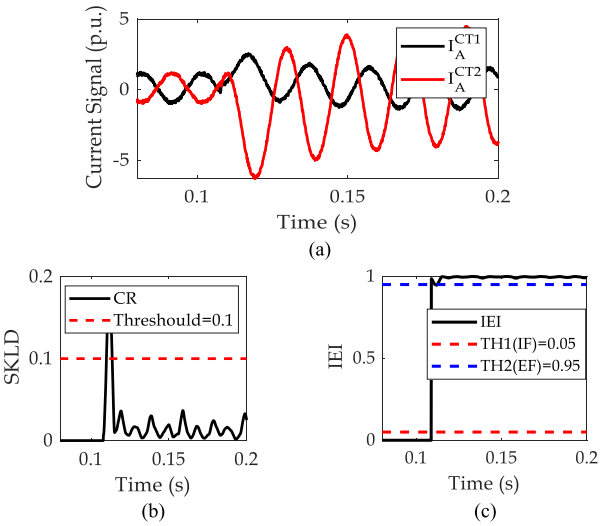

Fig. 14. Performance evaluation for external fault current signals using practical data. (a) CT current signals for external fault. (b) Proposed KLDI for external fault. (c) Proposed external/internal fault discrimination for external fault.

Fig. 14 demonstrates the performance evaluation for an external fault current signal, using practical data. As can be seen in Fig. 14(b), KLDI identifies the fault condition. However, as shown in Fig. 14(a), the current signals are almost 180° out of phase, and according to Fig. 14(c), the IEI index value is close to 1. As a result, the proposed index is able to detect external fault using the both KLDI and IEI indices.

C. Performance Comparison With State of the Art

In the following, the KLDI is compared with state of the art. In Table I, average response delay (ARD) and percent of correct identification (PCI) are provided.

TABLE I
RESPONSE TIME OF THE PROPOSED METHOD AND STATE-OF-THE-ART ALGORITHMS

		1	2	3	4	5
SHR	ARD (ms)	20.56	60.98	17.81	70.29	48.96
	PCI (%)	100	78	100	84	67
[23]	ARD (ms)	4.36	4.02	4.93	11.27	8.52
	PCI (%)	100	100	100	93	92
[25]	ARD (ms)	3.87	4.21	3.92	6.81	9.01
	PCI (%)	100	100	100	91	90
KLDI	ARD (ms)	3.24	3.97	3.12	4.62	4.01
	PCI (%)	100	100	100	100	98

The PCI is mathematically expressed as follows:

$$\mathrm{PCI} = \frac{\mathrm{NumberofCorrectIdentificationforCase}\ (X)}{\mathrm{Total\ Number\ of\ Case}\ (X)} \times 100 \tag{14}$$

where case (X) includes (case 1) 697 inrush, (case 2) 458 with remnant flux, (case 3) 1829 internal fault, (case 4) 964 internal fault with CT saturation, and (case 5) 150 inrush signals with internal fault cases.

From Table I, it is concluded that the following conditions hold.

1) In case 1, papers [23] and [25] and KLDI algorithms require a subcycle of data to perform their calculation, whereas SHR requires one cycle of data to achieve authenticated results.
2) In case 2, due to the reduction of the second harmonic content and SHR may fail to identify the inrush currents. However, papers [23] and [25] and KLDI algorithms can recognize the inrush current in case of remnant flux with high reliability.
3) In case 4, due to fast parameter estimation in the unsaturated region, KLDI has more immunity than [23], [25] and SHR algorithms in dealing with CT saturation conditions.
4) In case 5, comparing with the KLDI, SHR algorithms, and papers [23] and [25] have lower accuracy and higher delay time.

Overall, the comparison results indicate that the proposed algorithm is able to deal with challenging scenarios with high reliability, promising accuracy, and high speed.

V. CONCLUSION

This article introduced a similarity-based algorithm that discriminates the inrush and internal fault currents based on the discrepancy of the probability distributions of the reconstructed current and ideal sinusoidal signals. The proposed algorithm was validated under different internal/external faults and inrush currents obtained from simulation and practical data. It was observed that the proposed index is capable of recognizing internal fault signals with/without CT saturation in less than a quarter of a cycle. Applying different inrush currents to the proposed index, it was shown the proposed index is able to clearly recognize inrush current from the internal fault signal. The simulation and practical results showed that the proposed method has good immunity against noise. In the case of inrush with a minor internal fault, the proposed algorithm can successfully deal with

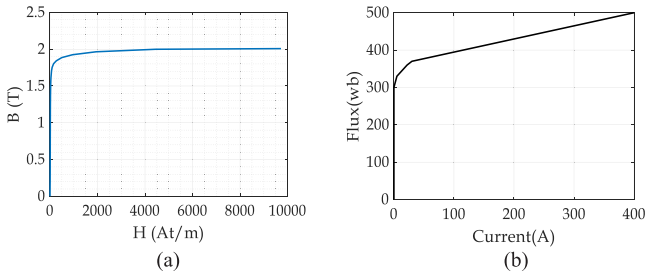

Fig. 15. Magnetization curves. (a) CT. (b) Transformer.

this scenario with a very good response delay. Also, the proposed algorithm has immunity against external fault with/without CT saturation. Comparing with the state-of-the-art algorithms, the KLDI has high accuracy and low response delay, and can be applied for the discrimination of the internal faults and inrush currents in power transformers.

Appendix

The parameters of the test system given in Fig. 2 are provided as given in Table II and Fig. 15 [31].

TABLE II
Specification of the Test System

Source	Vrated,1= 63 kV, Rth,1 =1.3(Ω), Lth,1= 0.042(H) Vrated,2= 63 kV, Rth,2 =1.12(Ω), Lth,2= 0.051(H)
Line	Positive Sequence Resistance (R) = 0.2710 Ohm/km Zero Sequence Resistance (R0) = 0.4760 Ohm/km Positive Sequence Reactance (X) = 0.3960 Ohm/km Zero Sequence Reactance (X0) = 1.3000 Ohm/km Positive Sequence Capacitance (C) = 0.0091 uF/km Zero Sequence Capacitance (C0) = 0.0072 uF/km
Transformer	Srated=30 MVA, 63/20- kV, Yg/Δ connection
CT	Primary: Ratio: 300:1, RCT1 = 1 Ω, LCT1 = 1 mH. Secondary: Ratio: 1000:1, RCT2 = 0.61 Ω, LCT2 = 0.9 mH

References

[1] S. H. Horowitz and A. G. Phadke, *Power System Relaying*, 3rd ed. Hoboken, NJ, USA: Wiley, 2008.

[2] M. E. H. Golshan, M. Saghaian-Nejad, A. Saha, and H. Samet, "A new method for recognizing internal faults from inrush current conditions in digital differential protection of power transformers," *Elect. Power Syst. Res.*, vol. 71, pp. 61–71, Sep. 2004.

[3] F. Haghjoo and M. Mostafaei, "Flux-based turn-to-turn fault protection for power transformers," *IET Gener. Transmiss. Distrib.*, vol. 10, pp. 1154–1163, Apr. 2016.

[4] G. Baoming, A. T. de Almeida, Z. Qionglin, and W. Xiangheng, "An equivalent instantaneous inductance-based technique for discrimination between inrush current and internal faults in power transformers," *IEEE Trans. Power Del.*, vol. 20, no. 4, pp. 2473–2482, Oct. 2005.

[5] M. Tripathy, R. P. Maheshwari, and H. K. Verma, "Application of probabilistic neural network for differential relaying of power transformer," *IET Gener. Transmiss. Distrib.*, vol. 1, pp. 218–222, Mar. 2007.

[6] H. Balaga, N. Gupta, and D. N. Vishwakarma, "GA trained parallel hidden layered ANN based differential protection of three phase power transformer," *Int. J. Elect. Power Energy Syst.*, vol. 67, pp. 286–297, May 2015.

[7] S. Afrasiabi, M. Afrasiabi, B. Parang, and M. Mohammadi, "Designing a composite deep learning based differential protection scheme of power transformers," *Appl. Soft Comput.*, vol. 87, Feb. 2020, Art. no. 105975.

[8] Z. Li, Z. Jiao, and A. He, "Knowledge-based artificial neural network for power transformer protection," *IET Gener. Transmiss. Distrib.*, vol. 14, pp. 5782–5791, Dec. 2020.

[9] D. Guillén, H. Esponda, E. Vázquez, and G. Idárraga-Ospina, "A new algorithm for transformer differential protection based on wavelet correlation modes," *IET Gener. Transmiss. Distrib.*, vol. 10, pp. 2871–2879, Sep. 2016.

[10] A. Roy, D. Singh, R. K. Misra, and A. Singh, "Differential protection scheme for power transformers using matched wavelets," *IET Gener. Transmiss. Distrib.*, vol. 13, pp. 2423–2437, Jun. 2019.

[11] A. Behvandi, S. G. Seifossadat, and A. Saffarian, "A new method for discrimination of internal fault from other transient states in power transformer using Clarke's transform and modified hyperbolic S-transform," *Elect. Power Syst. Res.*, vol. 178, Jan. 2020, Art. no. 106023.

[12] A. Rahmati and M. Sanaye-Pasand, "A fast WT-based algorithm to distinguish between transformer internal faults and inrush currents," *Eur. Trans. Elect. Power*, vol. 22, no. 4, pp. 471–490, Mar. 2011.

[13] M. H. Zendehdel and M. Sanaye-Pasand, "Development of two indices based on discrete wavelet transform for transformer differential protection," *Eur. Trans. Elect. Power*, vol. 22, no. 8, pp. 1078–1092, Aug. 2011.

[14] B. Noshad, M. Razaz, and S. G. Seifossadat, "A new algorithm based on Clarke's transform and discrete wavelet transform for the differential protection of three-phase power transformers considering the ultra-saturation phenomenon," *Elect. Power Syst. Res.*, vol. 110, pp. 9–24, May 2014.

[15] M. O. Oliveira, A. S. Bretas, and G. D. Ferreira, "Adaptive differential protection of three-phase power transformers based on transient signal analysis," *Int. J. Elect. Power Energy Syst.*, vol. 57, pp. 366–374, May 2014.

[16] A. Ngaopitakkul and C. Jettanasen, "A discrete wavelet transform approach to discriminating among inrush current, external fault, and internal fault in power transformer using low-frequency components differential current only," *IEEJ Trans. Elect. Electron. Eng.*, vol. 9, no. 3, pp. 302–314, Apr. 2014.

[17] P. Maya, S. Vidyashree, K. Roopasree, and K. P. Soman, "Discrimination of internal fault current and inrush current in a power transformer using empirical wavelet transform," *Proc. Technol.*, vol. 21, pp. 514–519, 2015.

[18] E. Ali, A. Helal, H. Desouki, K. Shebl, S. Abdelkader, and O. P. Malik, "Power transformer differential protection using current and voltage ratios," *Elect. Power Syst. Res.*, vol. 154, pp. 140–150, Jan. 2018.

[19] E. Ali, O. P. Malik, S. Abdelkader, A. Helal, and H. Desouki, "Experimental results of ratios-based transformer differential protection scheme," *Int. Trans. Elect. Energy Syst.*, vol. 29, pp. 1–14, Nov. 2019.

[20] E. Ali, O. P. Malik, A. Knight, S. Abdelkader, A. Helal, and H. Desouki, "Ratios-based universal differential protection algorithm for power transformer," *Elect. Power Syst. Res.*, vol. 186, Sep. 2020, Art. no. 106383.

[21] L. L. Zhang, Q. H. Wua, T. Y. Ji, and A. Q. Zhang, "Identification of inrush currents in power transformers based on higher-order statistics," *Elect. Power Syst. Res.*, vol. 9, pp. 146–161, May 2017.

[22] H. Weng, S. Wang, X. Lin, Z. Li, and J. Huang, "A novel criterion applicable to transformer differential protection based on waveform sinusoidal similarity identification," *Int. J. Elect. Power Energy Syst.*, vol. 105, pp. 305–314, Feb. 2019.

[23] H. Weng, S. Wang, Y. Wan, X. Lin, Z. Li, and J. Huang, "Discrete Fréchet distance algorithm based criterion of transformer differential protection with the immunity to saturation of current transformer," *Int. J. Elect. Power Energy Syst.*, vol. 115, pp. 105–114, Feb. 2020.

[24] T. Zheng, T. Huang, Y. Ma, Z. Zhang, and L. Liu, "Histogram-based method to avoid maloperation of transformer differential protection due to current-transformer saturation under external faults," *IEEE Trans. Power Del.*, vol. 33, no. 2, pp. 610–619, Apr. 2018.

[25] M. Tajdinian, M. Allahbakhshi, A. Bagheri, H. Samet, P. Dehghanian, and O. P. Malik, "An enhanced sub-cycle statistical algorithm for inrush and fault currents classification in differential protection schemes," *Int. J. Elect. Power Energy Syst.*, vol. 119, Jul. 2020, Art. no. 105939.

[26] A. M. Shah *et al.*, "Quartile based differential protection of power transformer," *IEEE Trans. Power Del.*, vol. 35, no. 5, pp. 2447–2458, Oct. 2020.

[27] R. G. Bainy and K. M. Silva, "Enhanced generalized alpha plane for numerical differential protection applications," *IEEE Trans. Power Del.*, vol. 36, no. 2, pp. 587–597, Apr. 2021.

[28] D. Bejmert, M. Kereit, F. Mieske, W. Rebizant, K. Solak, and A. Wiszniewski, "Power transformer differential protection with integral approach," *Int. J. Elect. Power Energy Syst.*, vol. 118, Jun. 2020, Art. no. 105859.

[29] S. Kullback, *Information Theory and Statistics*. Chelmsford, MA, USA: Courier Corporation, 1997.

[30] J. Pan, K. Vu, and Y. Hu, "An efficient compensation algorithm for current transformer saturation effects," *IEEE Trans. Power Del.*, vol. 19, no. 4, pp. 1623–1628, Oct. 2004.

[31] A. Sahebi and H. Samet, "Discrimination between internal fault and magnetising inrush currents of power transformers in the presence of a superconducting fault current limiter applied to the neutral point," *IET Sci., Meas. Technol.*, vol. 10, no. 5, pp. 537–544, Aug. 2016.

[32] N. Otsu, "A threshold selection method from gray-level histograms," *IEEE Trans. Syst., Man, Cybern.*, vol. SMC-9, no. 1, pp. 62–66, Jan. 1979.